Acta Tropica 237 (2023) 106729

Contents lists available at ScienceDirect

Acta Tropica

journal homepage: www.elsevier.com/locate/actatropica

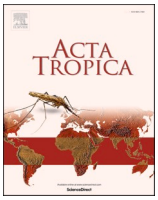

Camellia sinensis solvent extract, epigallocatechin gallate and caffeine confer trophocidal and cysticidal effects against *Acanthamoeba castellanii*

Lenu B. Fakae [a,b,c], Mohammad S.R. Harun [d], Darren Shu Jeng Ting [e], Harminder S. Dua [e,f], Gareth W.V. Cave [g], Xing-Quan Zhu [h], Carl W. Stevenson [b], Hany M. Elsheikha [a,*]

[a] Faculty of Medicine and Health Sciences, School of Veterinary Medicine and Science, University of Nottingham, Sutton Bonington Campus, Loughborough LE12 5RD, United Kingdom
[b] School of Biosciences, University of Nottingham, Loughborough LE12 5RD, United Kingdom
[c] Rivers State University, Nkpolu - Oroworukwo P.M.B 5080, Port Harcourt, Rivers, Nigeria
[d] Department of Biomedical Science, Advanced Medical and Dental Institute, Universiti Sains Malaysia, Bertam Campus, Kepala Batas, Pulau Pinang 13200, Malaysia
[e] Academic Ophthalmology, School of Medicine, University of Nottingham, Nottingham NG7 2RD, United Kingdom
[f] Department of Ophthalmology, Queen's Medical Centre, Nottingham NG7 2UH, United Kingdom
[g] School of Science and Technology, Nottingham Trent University, Nottingham NG11 8NS, United Kingdom
[h] Laboratory of Parasitic Diseases, College of Veterinary Medicine, Shanxi Agricultural University, Taigu, Shanxi 030801, China

ARTICLE INFO

Keywords:
Acanthamoeba castellanii
Acanthamoeba keratitis
Camellia sinensis
Amoebicidal effect
Epigallocatechin gallate
Caffeine

ABSTRACT

We examined the anti-acanthamoebic efficacy of green tea *Camellia sinensis* solvent extract (SE) or its chemical constituents against *Acanthamoeba castellanii* by using anti-trophozoite, anti-encystation, and anti-excystation assays. *C. sinensis* SE (625–5000 μg/mL) inhibited trophozoite replication within 24–72 h. *C. sinensis* SE exhibited a dose-dependent inhibition of encystation, with a marked cysticidal activity at 2500–5000 μg/mL. Two constituents of *C. sinensis*, namely epigallocatechin-3-gallate and caffeine, at 100 μM and 200 μM respectively, significantly inhibited both trophozoite replication and encystation. Cytotoxicity analysis showed that 156.25–2500 μg/mL of SE was not toxic to human corneal epithelial cells, while up to 625 μg/mL was not toxic to Madin-Darby canine kidney cells. This study shows the anti-acanthamoebic potential of *C. sinensis* SE against *A. castellanii* trophozoites and cysts. Pre-clinical studies are required to elucidate the *in vivo* efficacy and safety of *C. sinensis* SE.

1. Introduction

Acanthamoeba castellanii is an important parasitic agent that is capable of causing serious health conditions, including granulomatous amoebic encephalitis (Kofman and Guarner, 2022), *Acanthamoeba* keratitis (AK) (Carnt et al., 2020; Ting et al., 2021a, 2021b), and inflammation of the lungs and skin (Kofman and Guarner, 2022). Polyhexamethylene biguanide (PHMB) and chlorhexidine digluconate (Chx) are the treatments of choice for *Acanthamoeba* infections (Hadas et al., 2017a; Martín-Navarro et al., 2008). Because of the inadequate therapeutic effects of monotherapy with PHMB or Chx, their usage involves combination with diamidines; propamidine isethionate or hexamidine (Dart et al., 2009; Hay et al., 1994; Martín-Navarro et al., 2008). However, treatment failure and relapse do occur (Siddiqui et al., 2016). Oral miltefosine can be used as a salvage therapy for the treatment of AK, particularly in refractory cases and those with a significant burden of cysts (Avdagic et al., 2021; Thulasi et al., 2021). However, some patients may require multiple treatment courses and steroids to mitigate the inflammatory response encountered during the treatment (Thulasi et al., 2021; Si et al., 2022).

Alternative therapeutics have been suggested such as photodynamic chemotherapy (by employing the use of light-sensitive medication and a light source to destroy *A. castellanii*) (Ferro et al., 2006), therapeutic corneal cross-linking (by combining ultraviolet light A and riboflavin) (Khan et al., 2011; Said et al., 2021; Ting et al., 2021c), amniotic membrane transplantation (Ting et al., 2021d), silencing mRNA (Lorenzo-Morales et al., 2010), and combining nanoparticles with anti-*A. castellanii* drugs (Anwar et al., 2018). Due to therapeutic inadequacies and potential toxicity, researchers are delving into alternate sources of treatment using natural sources with anti-acanthamoebic

* Corresponding author.
E-mail address: Hany.Elsheikha@nottingham.ac.uk (H.M. Elsheikha).

https://doi.org/10.1016/j.actatropica.2022.106729
Received 18 September 2022; Received in revised form 19 October 2022; Accepted 19 October 2022
Available online 21 October 2022

activity (Dodangeh et al., 2018; Hadas et al., 2017a, 2017b; Kaya et al., 2019; Kaynak et al., 2018; Mahboob et al., 2017; Saoudi et al., 2017; Sifaoui et al., 2017).

Green tea brews, made from the leaves of the *Camellia sinensis* plant, have strong anti-acanthamoebic activity against the growth and encystation of *A. castellanii* (Fakae et al., 2020). Epigallocatechin-3-gallate (EGCG), a major component of *C. sinensis*, inhibits *A. castellanii* growth (Dickson et al., 2020). In addition to EGCG, *C. sinensis* contains catechin, epicatechin (EC), epicatechin-3-gallate (ECG), epigallocatechin (EGC), and caffeine, among other components. Catechins are flavonoids with antioxidant and antiviral capability, which is useful for the prevention of many diseases (Katada et al., 2020; Sanlier et al., 2018; Srichairatanakool et al., 2006; Yang et al., 2019; Zainuddin et al., 2022).

We have hypothesised that *C. sinensis* solvent extract (SE) can yield a higher concentration of phytochemicals from *C. sinensis* and better efficacies compared with *C. sinensis* brews. In the present study, we investigated the activity of *C. sinensis* SE against the trophozoites and cysts of *A. castellanii* and evaluated its cytotoxicity against human corneal (HCE-2) cells and Madin-Darby canine kidney (MDCK) cells. We also fractionated the main chemical ingredients of *C. sinensis* and tested their efficacy against trophozoites.

2. Materials and methods

2.1. Parasite culture

The *A. castellanii* strain of T4 genotype (American Type Culture Collection; ATCC 30,011) was used and maintained in peptone-yeast-glucose (PYG) medium as described previously (Fakae et al., 2020).

2.2. Solvent extraction of C. sinensis

C. sinensis SE was prepared using methanol and acetonitrile. Dried *C. sinensis* was ground to powder in a mill and weighed in large sized Whatman® cellulose extraction thimbles (Sigma-Aldrich, UK), which were plugged with cotton wool and placed in a Soxhlet apparatus. 500 mL of the solvent was poured through the thimble into a 1000 mL round bottom flask allowing for an initial extraction of the sample prior to the commencement of the extraction cycles. The Soxhlet apparatus was placed on a hotplate (Radley's Tech, Germany) at 70°C for methanol and 85°C for acetonitrile, and the SE was stirred by using a magnetic stirrer at 25xg. The SE was carried out for 48 h. Both SEs were pooled together and after cooling the suspensions were concentrated to dry matter using a vacuum with rotary evaporator (Rotavapor® R-300,BUCHI, Flawil, Switzerland) and a water bath set to 40°C.

2.3. Preparation of SE solutions for testing

C. sinensis SE solution was prepared at a stock concentration of 10,000 μg/mL containing 0.025% DMSO. The solution was filtered through a 0.22 μm pore size Millipore syringe filter (MILLEX®-HA brand, Ireland). Two-fold serial dilutions of *C. sinensis* SE (5000 μg/mL - 156.25 μg/mL) were prepared using PGY as a diluent. For the cytotoxicity assays, *C. sinensis* serial dilutions (v/v) were prepared as described above using the respective cell culture medium as the diluent.

For *C. sinensis* encystation medium, a stock concentration of 10,000 μg/mL was achieved by preparing a SE solution as described above but using distilled water instead of PGY medium. For the hyperosmotic encystation media, 10 g of glucose monohydrate, 0.48 g of magnesium chloride (Sigma-Aldrich) and one phosphate-buffered saline (PBS) tablet (Gibco®, Life technologies, ThermoFisher Scientific, UK) were dissolved in 100 mL of the distilled water-*C. sinensis* SE solution. This was stirred on a magnetic stirrer for 30 min and the suspension was filtered into a sterile bottle using a 0.45 μL Millipore syringe filter. The standardized encystation solution (negative control) was prepared using distilled water. The positive control included standardized encystation solution supplemented with 5% of the encystation inhibitor phenylmethylsulfonyl fluoride (PMSF) solution (Sigma Life Science, Switzerland).

2.4. Cytotoxicity tests

HCE-2 cells (CRL11135, ATCC, Manassas, Virginia, USA) were seeded into a Thermo Scientific™ Nunc MicroWell 96-well plate (ThermoFisher Scientific, Loughborough, UK) at 7.5×10^3 cells/well and grown to 80–90% confluency in the presence of growth media as described previously (Bagshaw et al., 2020). HCE-2 cells were subsequently incubated with a 1:2 serial concentration of *C. sinensis* starting from 5000 μg/mL to 156.3 μg/mL for 48 h. The culture medium was used as a negative control. The lactate dehydrogenase (LDH) assay (ThermoFisher Scientific, UK) was performed as per the manufacturer's instructions. At 24 h and 48 h post-treatment, 50 μl of supernatant was obtained from each well and $OD_{490–680}$ was measured using a BMG Clariostar microplate reader (BMG LABTECH Ltd., Aylesbury, United Kingdom). Cytotoxicity (%) was calculated using the following formula: $[((I_{treatment} - I_{NC}) / (I_{PC} - I_{NC})) \times 100$; I = intensity].

MDCK cells were seeded in 96-well microplates at a density of 5×10^3 cells/well in 100 μl Gibco Dulbecco's Modified Eagle Medium (DMEM) (Gibco®, Life technologies, ThermoFisher Scientific, UK). After 48 h of incubation in a humidified atmosphere of 5% CO_2 at 37 °C, the medium was removed, and the cultures were treated with the SE at the same above-mentioned concentrations and incubated for 3, 24, and 48 h. Parallel negative control wells contained MDCK cells with the respective medium only, without *C. sinensis*. The positive control included wells treated with 3% sodium dodecyl sulfate (SDS). At each time point of incubation, cell proliferation was determined using the sulforhodamine B (SRB) assay as described previously (Ortega-Rivas et al., 2016).

2.5. Evaluation of the trophocidal activity

Trophozoites (3.2×10^5) were treated with SE (5000, 2500, 1250, and 625 μg/mL). Controls included an equal number of trophozoites in PYG only (negative control) or in PYG supplemented with 0.02% Chx (positive control). After 24, 48 and 72 h, trophozoites were counted using a hemocytometer (Neubauer-improved bright line, Marienfeld, Germany) and a CETI inverted microscope (Medline Scientific, UK) to determine the effect of each treatment on the growth rate of trophozoites.

2.6. Selectivity index

The *C. sinensis* SE concentration that caused 50% inhibition of cell growth was expressed as 50% cytotoxic concentration (CC_{50}). The CC_{50} of *C. sinensis* on HCE-2 and MDCK cells was calculated by plotting dose-response curves followed by linear regression analysis using Graph Pad Prism 7 software. The calculation of half-maximal inhibitory concentration (IC_{50}), which is the concentration of SE that caused a 50% reduction in the growth of trophozoites compared to the control, was performed using nonlinear regression (curve fit) built-in analysis tool of dose-response inhibition (three parameters). The selectivity index (SI) represents the ratio of the CC_{50} for host cells to the IC_{50} for *A. castellanii* and was calculated by comparing the cytotoxicity of *C. sinensis* on HCE-2 cells and MDCK cells to the activity against the trophozoites.

2.7. Effects of transient exposure on trophozoites

3×10^5 trophozoites were treated with SE (5000, 2500, 1250, and 625 μg/mL), with PYG medium as a negative control, and 0.02% Chx in PYG as a positive control. After 2 and 24 h, trophozoites were washed twice with PYG medium to remove traces of *C. sinensis*. Then, trophozoites were suspended in 5 mL of fresh PYG, in T25 tissue culture flasks,

and incubated. After 24, 48 and 72 h, the number of trophozoites was counted using a hemocytometer to determine the growth inhibitory effect of treatment on trophozoites. The trophozoites were also examined using a Leica DMIL CMS inverted microscope (Germany) with a Leica Application Suite (LAS version 4.3) to identify any morphological alterations caused by *C. sinensis*.

2.8. Inhibitory effect of C. sinensis on cyst formation

Trophozoites (6×10^5) were treated with *C. sinensis* SE hyperosmotic solution (5000, 2500, 1250, and 625 μg/mL). The negative control included trophozoites treated with hyperosmotic encystation medium. The positive control included trophozoites treated with hyperosmotic encystation medium plus 5% PMSF solution. The encystation rate was determined by counting the number of trophozoites versus cysts for each concentration after 24, 48 and 72 h of treatment using a hemocytometer. After 72 h, the cultures were treated with 0.5% SDS and left for 60 min to digest any remaining trophozoites. Then, pre-, and post-SDS treatment counts were performed and the encystment percentage was determined using the formula:

$$\%encystment = post - digestionnumber/pre - digestionnumber \times 100.$$

2.9. Inhibitory effect of C. sinensis on excystation

2×10^5 cysts were treated with 5000, 2500, 1250, and 625 μg/mL. The negative control included cysts in PYG only, while the positive control included cysts in PYG supplemented with 0.02% Chx. After incubation for 24, 48 and 72 h, we determined the cyst to trophozoite excystation ratio using a hemocytometer and a CETI inverted microscope. The treated cysts were also examined using a Leica DMIL CMS inverted microscope with a Leica Application Suite to identify morphological alterations during excystation caused by exposure to treatment.

2.10. Scanning electron microscopy (SEM)

Trophozoites and cysts treated with SE were harvested, fixed, and dehydrated using a graded series of ethanol. Sample processing was performed as described previously (Fakae et al., 2020). Images were obtained with varying magnifications using a JEOL JSM-7100F LV Scanning Electron Microscope (JOEL, Tokyo, Japan).

2.11. Partitioning of C. sinensis SE using chromatography

A sample of *C. sinensis* SE was analyzed by flash column chromatography using Puriflash 5.125Plus (Interchim, Montluçon, France) to identify the fractions in *C. sinensis* SE. To identify which method separates more fractions, two runs were conducted with different combinations of solvents as mobile phases. The first mobile phase included 0.1% formic acid in water and water + 0.1% formic acid in methanol, while the second mobile phase included 0.2% acetic acid in water + acetonitrile at a 91:9 ratio and water + acetonitrile at a 20:80 ratio. Two flash columns were used; puriflash C18HC spherical silica flash II column with particle size 50 μm and puriflash C18HP spherical silica flash II column.

2.12. HPLC profiling of C. sinensis SE

C. sinensis SE fractions were characterized using ultra-high performance liquid chromatography quadrupole time of flight tandem mass spectrometry (UHPLC-QTOF-MS) (Waters, Milford, MA, USA) to identify the analytes present in these fractions. A Restek C18 Raptor™ column (Restek Thames, High Wycombe, UK) was used. The chromatographic data were analyzed, and chemical composition of each component was confirmed by matching the chemical formula with references in the library of MassLynx® software (version 4.1, Waters, Milford, MA, USA).

2.13. Inhibitory effects of C. sinensis constituents on trophozoites

Ten *C. sinensis* components, namely theogallin, theobromine, EGC, caffeine, ECG, EGCG, EC, catechin, kaempferol, and myricetin identified in *C. sinensis* by HPLC profiling, were purchased from Sigma-Aldrich (UK). Stock solutions of each compound were prepared with PGY to a final concentration of 1000 μM. Two-fold serial dilutions of each compound (200 μM–3.12 μM) were used to investigate their inhibitory effect on the growth of trophozoites using the SRB assay. We also tested the efficacy of the 10 compounds combined at an equal ratio. In another experiment, we combined the two most potent compounds to determine any synergist effect. At 3, 6, 24, 48 and 72 h post-incubation, the color absorbance of each well was measured as previously described (Fakae et al., 2020; Ortega-Rivas et al., 2016).

2.14. Inhibitory effect of C. sinensis constituents on encystation

Trophozoites (6.2×10^5) were treated with 500, 250, 125, and 62.5 μM of encysting solutions containing EGCG, theobromine, or EGCG-theobromine mixed in a 1:1 ratio. The negative and positive controls were the same as described in encystation experiments above.

2.15. Statistical analysis

All experiments were performed in technical triplicate and in three independent experiments. All statistical analyses were performed using GraphPad Prism Version 9.0.0 (GraphPad Software Inc., CA USA). One-way and two-way analysis of variance (ANOVA) with Turkey's multiple comparison test were used to compare groups. The results are expressed as mean ± standard error of mean (SEM). $p < 0.05$ was considered statistically significant.

3. Results

3.1. Cytotoxicity against mammalian cells

HCE-2 cells were exposed to SE at doses of 156.25–5000 μg/mL (Fig. 1a). By 24 h post-treatment, no significant differences were observed in the toxicity between control and treated cells at concentrations 156.25–1250 μg/mL ($p > 0.99$). However, 2500 μg/mL and 5000 μg/mL concentrations showed a significant increase in toxicity compared with the negative control ($p = 0.0129$ and $p < 0.0001$, respectively). At 48 h, 156.25–2500 μg/mL showed no significant difference to the negative control ($p > 0.99$). However, 5000 μg/mL showed a significant increase in cytotoxicity compared with the control (Fig. 1a). The cytotoxicity observed with 2500 μg/mL at 24 h could be transient because toxicity had dropped at 48 h. MDCK cells treated with 156.25–5000 μg/mL showed an increase in cell replication, although the rates were significantly lower than the negative control ($p < 0.0001$), suggesting cytotoxicity caused by *C. sinensis* (Fig. 1b).

3.2. Inhibitory effects of C. sinensis SE on trophozoites

At 24 h post-treatment, comparisons of treatment groups with negative control (PGY treatment), vehicle control (PGY+DMSO), and positive control (Chx) showed an increase in the number of trophozoites exposed to 312.5 μg/mL ($p < 0.0001$) (Fig. 2a). However, the higher concentrations, 625–5000 μg/mL, showed a significant decrease in trophozoite numbers compared to the negative control ($p < 0.0001$). At 48 h, trophozoites treated with 312.5 μg/mL continued to grow with no significant difference from the negative (PGY) and vehicle (PGY+DMSO) controls ($p = 0.0862$). At 72 h post-treatment, 312.5 μg/mL still showed increase in trophozoites, while higher concentrations showed a decrease in trophozoites with no significant difference

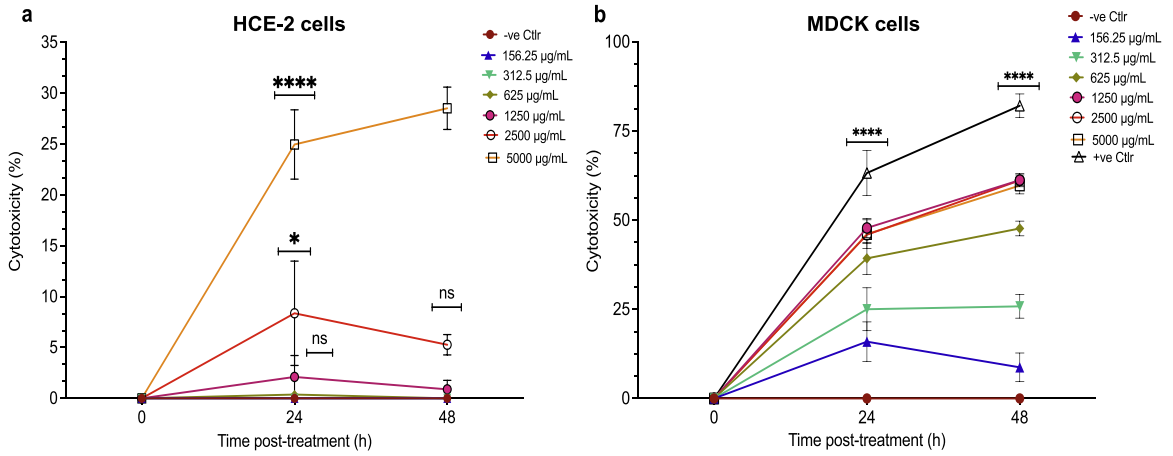

Fig. 1. *The toxicity of C. sinensis SE on cultured human corneal epithelial (HCE-2) and Madin-Darby Canine Kidney (MDCK) cells*. Cultured cells were exposed to the indicated concentrations and cytotoxicity was investigated using the lactate dehydrogenase and Sulforhodamine B assays for (a) HCE-2 cells and (b) MDCK cells respectively. **** $p < 0.0001$; ns, non-significant.

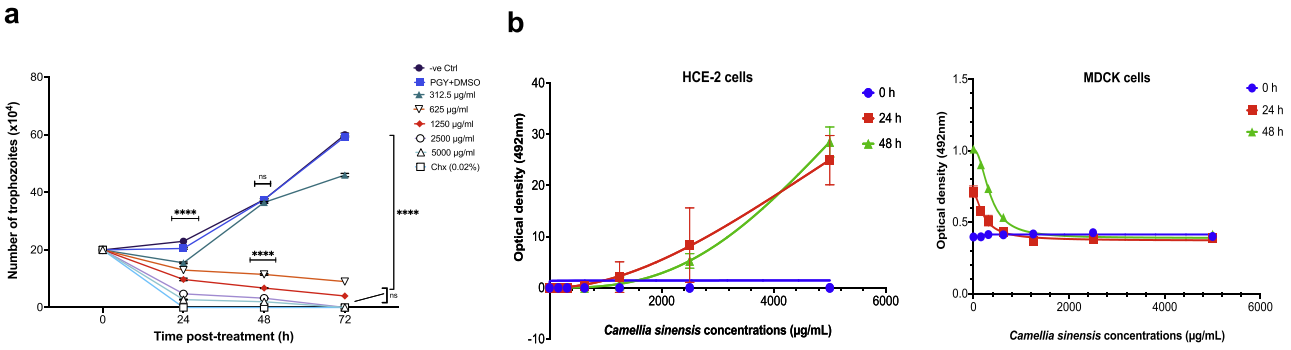

Fig. 2. *Inhibitory effects and selectivity of C. sinensis SE on A. castellanii trophozoites*. (a) Growth inhibitory effect of *C. sinensis* on *A. castellanii* trophozoites at 24, 48, and 72 h post-treatment doses of 312.5–5000 µg/mL. (b) The CC_{50} of *C. sinensis* SE on HCE-2 cells (left) and MDCK cells (right). ****, $p < 0.0001$; ns, non-significant.

between these higher doses. The effect of the two highest does, 2500 µg/mL and 5000 µg/mL, was comparable to the effect of the positive control as they completely eradicated trophozoites ($p > 0.99$).

3.3. Selectivity index of *C. sinensis* SE

The IC_{50} of *C. sinensis* SE against trophozoites was 1309 ± 517.1 µg/mL at 24 h and 409 ± 8.09 µg/mL at 48 h. The CC_{50} for HCE-2 cells and MDCK cells was 8891 ± 1135 µg/mL at 24 h and 6916 ± 199 µg/mL at

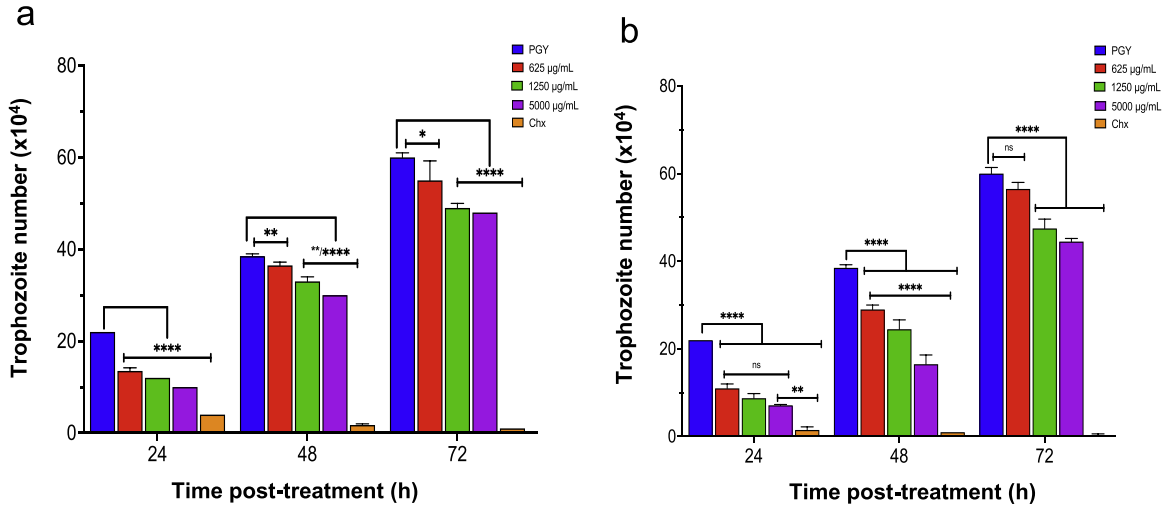

Fig. 3. *Transient effect of C. sinensis SE on A. castellanii trophozoites*. Growth inhibition of *A. castellanii* trophozoites post-transient exposure to 625 µg/mL, 1250 µg/mL, and 5000 µg/mL of *C. sinensis* and chlorhexidine (Chx) for 2 h (a) and 24 h (b). Significant decrease was detected between Chx and the concentrations of *C. sinensis* SE at 72 h post-exposure at both time points. **, $p = 0.0058$; ****, $p \leq 0.0001$; ns, non-significant.

48 h, and 222.1 ± 25.06 μg/mL at 24 h and 346.3 ± 12.89 μg/mL at 48 h, respectively (Fig. 2b). The SI for *C. sinensis* was calculated as the ratio CC_{50} on HCE-2 cells and MDCK cells to IC_{50} against trophozoites. *C. sinensis* had a *C. sinensis* has selective cytotoxicity for *A. castellanii* with a SI = 6.8 at 24 h and SI = 16.9 at 48 h, when tested against HCE-2 cells. However, *C. sinensis* had a SI = 0.17 and SI = 0.85, when tested against MDCK cells at 24 h and 48 h, respectively. These results demonstrate the lower sensitivity of HCE-2 cells, compared to MDCK cells, to *C. sinensis* treatment.

3.4. Effect of transient exposure

At 2 h post-exposure, there was a significant decrease ($p < 0.05$) in the parasite growth inhibition caused by Chx compared with treatment with 625 μg/mL, 1250 μg/mL, and 5000 μg/mL (Fig. 3a). Likewise, for 24 h exposure there was a significant decrease ($p < 0.05$) between the parasite growth inhibition caused by Chx and the three concentrations. *C. sinensis* at the three concentrations did not sustain trophozoite growth inhibition after a transient exposure of 2 h and 24 h (Fig. 3b). For 2 h and 24 h exposure, despite the significant increase in trophozoite numbers between negative control and *C. sinensis* concentrations ($p < 0.0001$), there was continuous replication of the trophozoites between 24 h and 72 h.

3.5. C. sinensis SE inhibits encystation

One-way ANOVA revealed significant dose-dependent effects of *C. sinensis* on the encystation rate pre-SDS digestion ($p < 0.0001$) and post-SDS digestion ($p < 0.0001$) (Fig. 4a). We detected 100% inhibition rate with 2500 μg/mL and 5000 μg/mL encystation buffer ($p < 0.0001$). Likewise, 1250 μg/mL caused a significant decrease in encystation compared to the negative control ($p < 0.01$). On the other hand, no significant difference was detected in encystation inhibition between the lowest concentration of 625 μg/mL and the negative control (Fig. 4b).

3.6. C. sinensis extract interferes with excystation

Cysts exposed to 312.5–5000 μg/mL were examined to determine cyst: trophozoite ratio at 72 h post exposure (Fig. 5a). There was a significant dose-dependent decrease in excystation ($p < 0.0001$), with an absolute inhibition of excystation at 1250 - 5000 μg/mL (Fig. 5a). Similarly, the higher concentrations of 1250 - 5000 μg/mL displayed 100% inhibition of excystation, mimicking the activity of Chx ($p > 0.05$) (Fig. 5b). Although there were significant increase in inhibition of excystation between the higher concentrations and the lower concentrations of 312.5 and 625 μg/mL, these low concentrations exhibited 78% and 87% inhibition of excystation respectively, with a significant increase from the negative control ($p < 0.0001$).

3.7. Morphological changes after exposure to C. sinensis SE during excystation

Microscopic observation of cysts 72 h post-exposure to *C. sinensis* SE showed extensive excystation of the negative control. While cysts exposed to *C. sinensis* SE exhibited mild to extensive damage as shown by the presence of damaged cysts, with cytosol contents in the culture media, suggesting cytolysis (Fig. S1). With increasing *C. sinensis* concentrations, the amount of cellular debris increased.

3.8. Ultrastructural features of active and encysting trophozoites

SEM micrographs of trophozoites (Fig. 6) revealed rupture of the plasma membrane, shrunken cytosol and changes in size. *C. sinensis* SE caused complete destruction of trophozoites similar to Chx. The trophozoites in the control samples appeared encysting and cysts were held together. In contrast, exposure of encysting trophozoites to SE caused loss of their adhesive properties and breaking up of the cysts. After 72 h exposure, there was extensive destruction of the encysting and encysted trophozoites (Fig. 7).

3.9. Chromatographic profile of C. sinensis SE

The first mobile phase (acetic acid + acetonitrile) revealed 6 fractions of *C. sinensis* SE (Fig. S2), while from the second mobile phase (Fig. S3) 10 fractions were identified. The identified 10 components in *C. sinensis* SE are listed in Table 1.

3.10. Trophocidal effects of C. sinensis components

The growth inhibitory effect of the 10 *C. sinensis* components (Table 1) on trophozoites was examined at doses of 3.125 μM, 6.25 μM, 12.5 μM, 25 μM, 50 μM, 100 μM and 200 μM at 24, 48, and 72 h post treatment. For EGCG, at 24 h post- treatment, all the treatment groups showed no trophozoite growth with no significant difference compared with positive control ($p > 0.05$). This inhibitory effect was sustained at 48 and 72 h only for samples treated with 100 μM and 200 μM concentrations (Fig. 8a). For caffeine, at 24 h, the treatment groups showed no growth with no significant difference in the trophozoite number compared with the positive control ($p > 0.05$). However, at 48 h all concentrations showed growth of trophozoites, though with significance difference from the PGY control. After 48 h, all the concentrations except for 3.125 μM and 6.25 μM exhibited decline of trophozoite

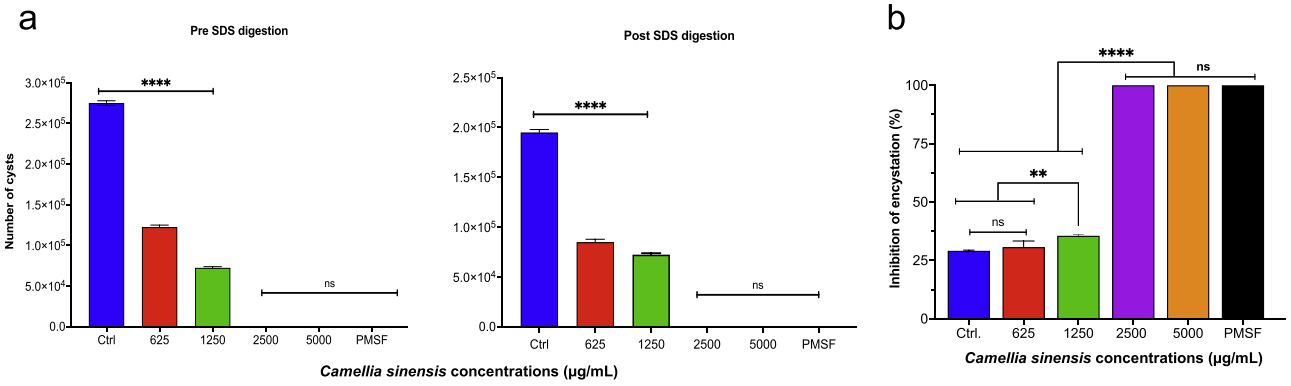

Fig. 4. *Effect of Camellia sinensis SE on encystation.* (a) At 72 h post-synchronized encystation, pre- and post-SDS digestion, 2500–5000 μg/mL *C. sinensis* showed no cysts with no significant difference between the positive control (5 mM PMSF). The lower doses of 625–1250 μg/mL showed some level of encystation but with a significant decrease compared with the negative control ($p < 0.0001$). (b) Percentage inhibition of encystation of *A. castellanii* compared with the positive control (5 mM PMSF). ****, $p < 0.0001$; ns, non-significant.

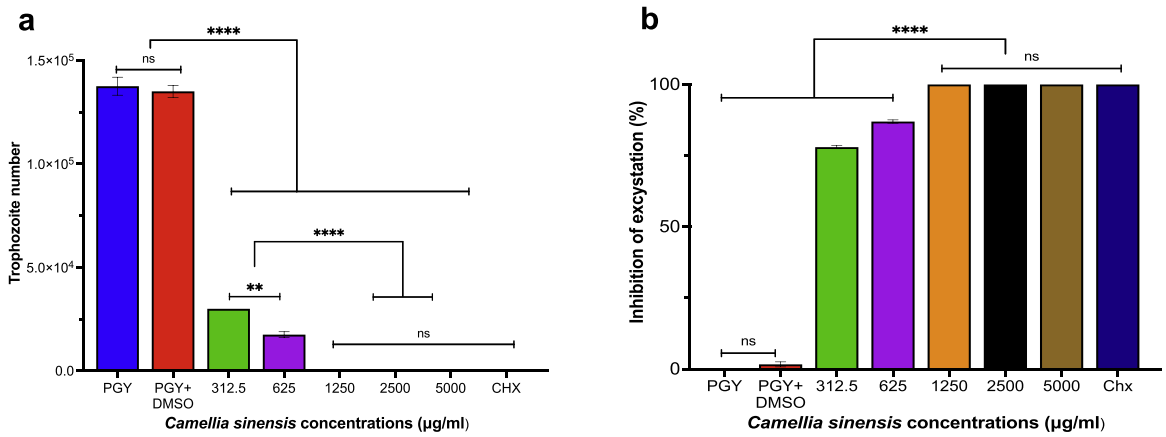

Fig. 5. *Effects of C. sinensis SE on excystation at 72 h post-exposure to the indicated concentrations.* (a) The concentrations of 1250–5000 µg/mL exhibited 100% inhibition of excystation, similar to chlorhexidine (Chx). (b) Percentage of trophozoite excystation in *C. sinensis* SE. Exposure to 1250–5000 µg/mL exhibited 100% inhibition of excystation, similar to Chx. ****, $p < 0.0001$; ns, non-significant.

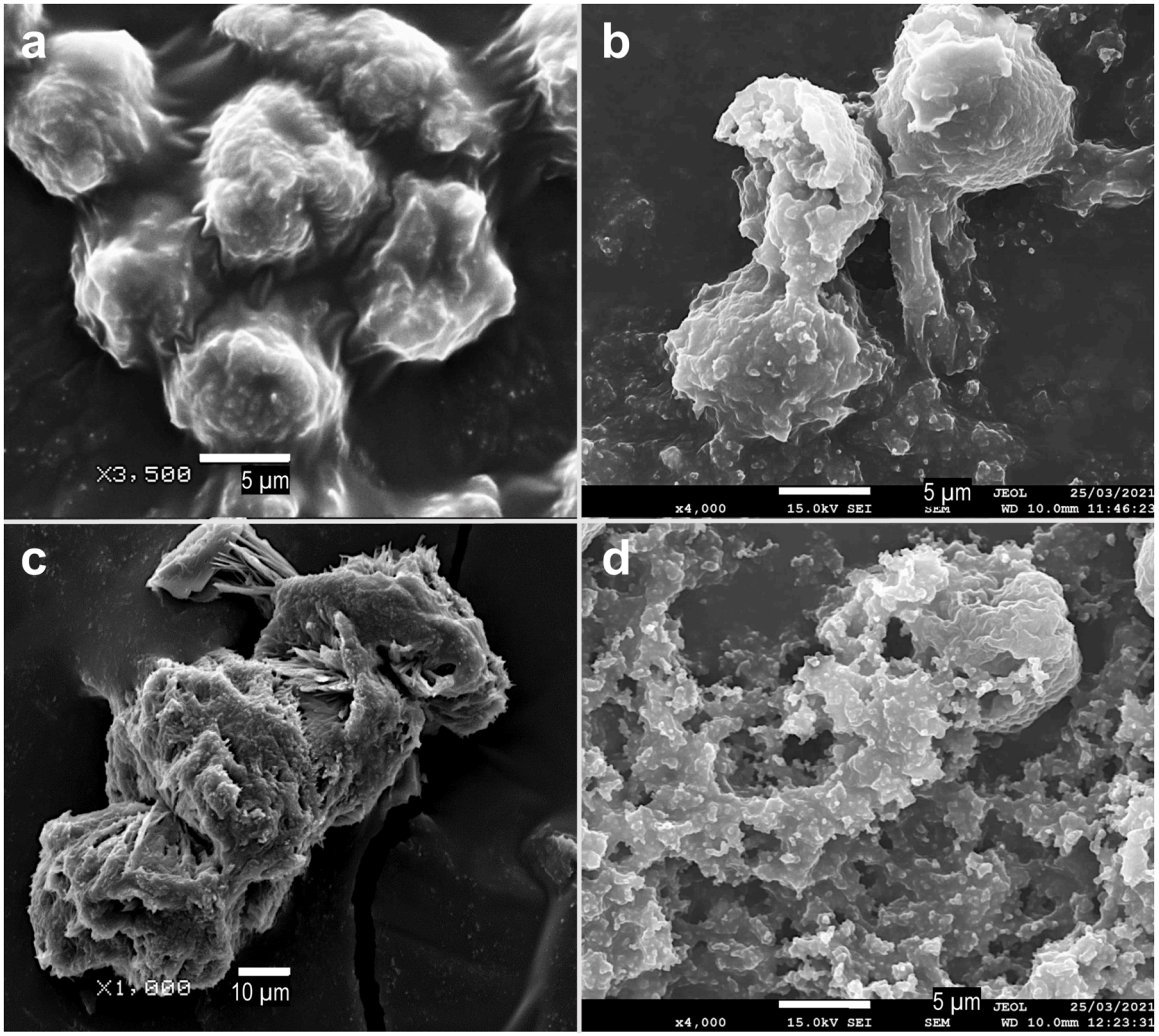

Fig. 6. *Representative scanning electron microscopy (SEM) micrographs of A. castellanii trophozoites exposed to C. sinensis SE, showing loss of membrane of trophozoites and shrinking of their size.* Continued exposure to both *C. sinensis* SE and chlorhexidine (Chx) showed loss of acanthopodia and progressive destruction of trophozoites. (a) Trophozoites in PGY (control) attached together by adhesin; (b) Trophozoites in 2500 µg/mL of *C. sinensis* SE at 24 h showing loss of protective adhesin and progressive destruction of the trophozoites. (c) Trophozoites in Chx at 24 h showing loss of protective adhesin and shrinking/destruction of trophozoites. (d) Trophozoites in 2500 µg/mL of *C. sinensis* SE at 72 h showing complete destruction of the trophozoites with some parasite debris in the background. Magnifications: X3500, X4000, X1000, and X4000 respectively. Scale bars, 5, 1,10, and 1 µm, respectively.

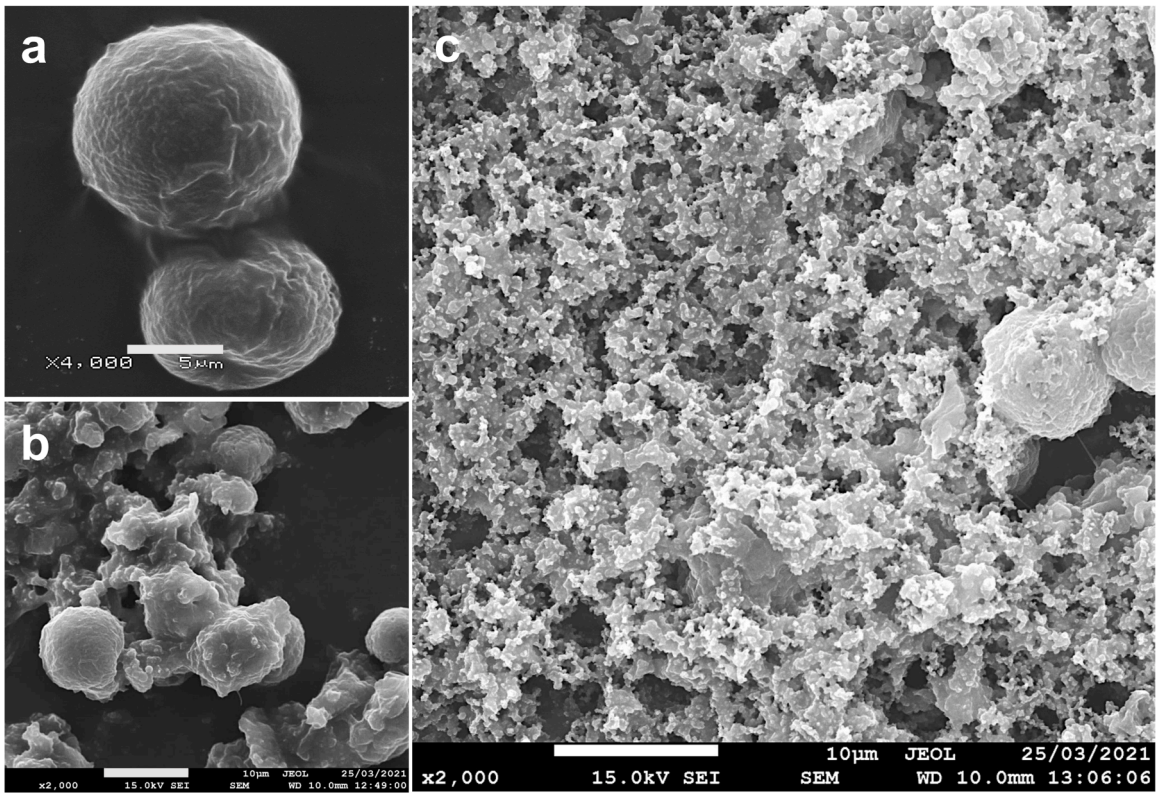

Fig. 7. *Representative scanning electron microscopy (SEM) micrographs showing destruction of A. castellanii cysts exposed to C. sinensis SE.* (a) Cysts in the control encystation buffer adhered together; (b) Aggregated cysts exposed to *C. sinensis* 625 μg/mL at 72 h showing a number of broken cysts, cyst debris and a few intact cysts; (c) Cysts exposed to *C. sinensis* 2500 μg/mL for 72 h showed extensive destruction. Magnifications: X4,000, X2,000, and X4,000, respectively. Scale bars, 5, 10, and 10 μm, respectively.

Table 1
Chemical constituents of *C. sinensis* SE analyzed by UHPLC–QTOF–MS.

Compound	Molecular Formula	*m/z* ratio	Chemical class
Theogallin	$C_{14}H_{16}O_{10}$	344.27	Polyphenol
Theobromine	$C_7H_8N_4O_2$	180.164	Xanthine Alkaloid
Epigallocatechin	$C_{15}H_{14}O_7$	306.27	Flavonoid
Caffeine	$C_8H_{10}N_4O_2$	194.19	Methylxanthine alkaloid
Epicatechin Gallate	$C_{22}H_{18}O_{10}$	442.37	Flavonoid
Epigallocatechin Gallate	$C_{22}H_{18}O_{11}$	458.37	Polyphenol
Epicatechin	$C_{15}H_{14}O_6$	290.27	Polyphenol/ catechin
Catechin	$C_{15}H_{14}O_6$	290.27	Flavonoid
Kaempferol	$C_{15}H_{10}O_6$	286.23	Flavonoid
Myricetin	$C_{15}H_{10}O_8$	318.24	Flavonoid

growth with the 100 μM and 200 μM concentrations mirroring the effect of the positive control at 72 h to eliminate the trophozoites ($p > 0.05$) (Fig. 8b). Although there were significance differences between ECG, EGC, EC, and catechin and negative control, they all exhibited little or no inhibition of trophozoite growth from 24 h to 72 h (Fig. 8c–f). For theobromine, myricetin, theogallin, and kaempferol, there was no inhibition to trophozoite growth from 24 h to 72 h post-treatment with all doses (Fig. 8g–j). There was no synergistic activity of *C. sinensis* components as their combination exhibited no inhibition of trophozoite growth (Fig. S4).

3.11. Cysticidal effect of C. sinensis ingredients

We detected 100% trophozoite encystation inhibition of all tested concentrations of *C. sinensis* ingredients, with no significant difference between them and the positive control ($p < 0.0001$) (Fig. S5).

4. Discussion

We examined the anti-acanthamoebic efficacy of *C. sinensis* SE and its individual components. We evaluated the toxicity of *C. sinensis* SE on HCE-2 and MDCK cells in vitro. *C. sinensis* exhibited a dose-dependent toxic effect on MDCK cells, particularly at concentrations 1250–5000 μg/mL. HCE-2 cells, in contrast, exhibited only 30% cytotoxicity even at 5000 μg/mL up to 48 h post exposure. Next, we demonstrated the anti-acanthamoebic activity of *C. sinensis* SE against trophozoites and cysts. The concentrations 625–5000 μg/mL exhibited a sustained and progressive inhibition of trophozoite replication and cytolysis. The lower concentrations 625–1250 μg/mL slightly inhibited encystation, while higher concentrations, 2500–5000 μg/mL, completely inhibited trophozoite-to-cyst differentiation. In addition to inhibition of encystation, *C. sinensis* SE caused the destruction of trophozoites. Electron microscopic analysis showed that *C. sinensis* SE resulted in considerable damage, including rupture of plasma membrane and disruption of the adhesin. Light microscopic analysis showed extensive destruction of *A. castellanii* at 72 h post-exposure. Although a combination of the 10 *C. sinensis* bioactive compounds did not yield favourable anti-acanthamoebic activity, EGCG and caffeine individually inhibited trophozoite replication within a concentration range of 3.125–200 μM. Interestingly, theobromine inhibited cyst to trophozoite differentiation during excystation even at 62.5 μM. Also, a combination of theobromine and EGCG inhibited encystation.

It is intriguing that exposure of trophozoites to 312.5 μg/mL, which did not inhibit trophozoite replication, inhibited excystation and destroyed cysts and trophozoites during excystation. Although *A. castellanii* can encyst upon exposure to adverse conditions,

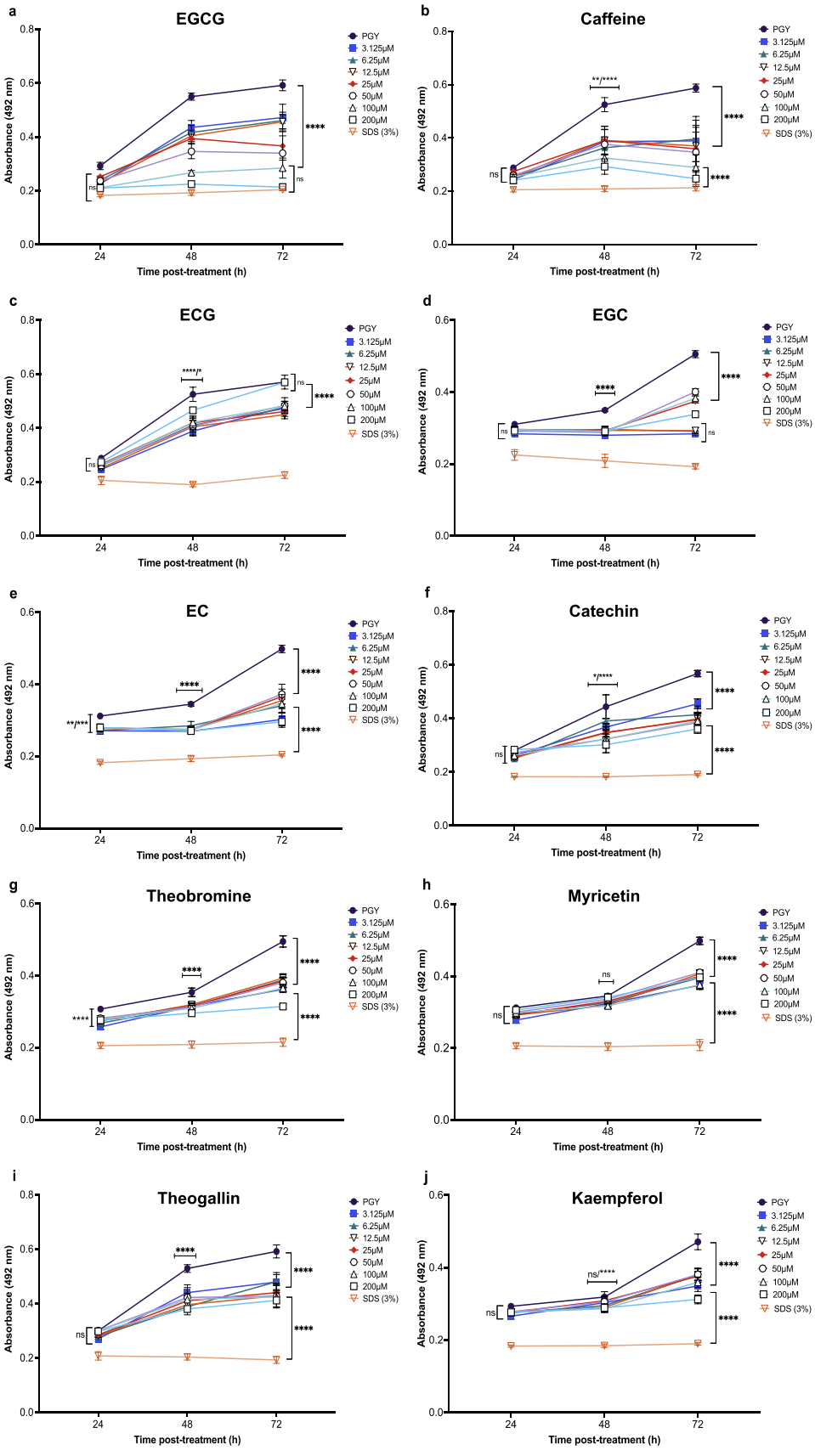

Fig. 8. *Growth inhibitory effect of C. sinensis chemical constituents on A. castellanii at 24, 48, and 72 h post-treatment with the indicated concentrations*. (a) Epigallocatechin-3-gallate (EGCG) at 48 and 72 h post-exposure. The PGY group showed a significant increase in trophozoite viability, while at 72 h, 100–200 μM EGCG-treated groups showed no significant difference with the positive control (SDS), indicating that both groups successfully inhibited trophozoite replication. (b) Caffeine at 100 μM and 200 μM exhibited the same trend. (c-f). All treatment groups (epicatechin-3-gallate (ECG), epigallocatechin (EGC), epicatechin (EC), and catechin, respectively) showed significant decrease in trophozoite growth compared to the negative control at 48 and 72 h post-exposure. (g–j) All treatment groups (theobromine, myricetin, theogallin, and kaempferol, respectively) showed significant decrease compared to the negative control (PGY) and to the SDS at 48 and 72 h post exposure. Despite the differences these constituents did not exhibit sustained anti-acanthamoebic capability from 48 h post-treatment, as shown by SDS. ****, $p \leq 0.0001$; ns: non-significant.

trophozoites might not have the ability to halt and reverse the excystation process in the presence of *C. sinensis*. This disruption in phenotypic differentiation may have activated a proapoptotic pathway and induced death of excysting trophozoites.

EGCG has anti-acanthamoebic activity (Dickson et al., 2020) and antifolate activity against *Stenotrophomonas maltophilia* (Navarro-Martínez et al., 2005), via inhibition of dihydrofolate reductase (DHFR), which is involved in nucleotide biosynthesis. *A. castellanii* has DHFR and antifolate trimethoprim drug has amoebicidal activity (Siddiqui et al., 2016). Thus, inhibition of DHFR by EGCG can disrupt DNA synthesis in *A. castellanii*. EGCG can also inhibit protein synthesis and induce apoptosis in pancreatic cancer cells (Shankar et al., 2007). It is therefore conceivable that EGCG may contribute to the anti-acanthamoebic effects of *C. sinensis* via its antifolate and protein synthesis inhibitory activities. *A. castellanii* secretes many serine protease and metalloprotease (Khan, 2006), which compromise cell membrane integrity and cause cytolysis (Dudley et al., 2008). These enzymes regulate encystation (Alsam et al., 2005; Lorenzo-Morales et al., 2015). EGCG can inhibit serine proteases and metalloproteases (Benelli et al., 2002; Wyganowska-Świątkowska et al., 2018) and increase the expression of tissue factor pathway inhibitor-2 (TFPI-2), a Kunitz-type serine proteinase inhibitor (Gu et al., 2009). Hence, EGCG, via inhibition of these enzymes may have caused cytolysis of trophozoites and inhibited encystation.

In conclusion, *C. sinensis* SE had amoebicidal activities against trophozoite and cyst forms of *A. castellanii*. Although a combination of *C. sinensis* components did not exhibit amoebicidal ability, EGCG, caffeine and theobromine completely inhibited trophozoite encystation. Additionally, EGCG and caffeine had amoebicidal ability against both forms of *A. castellanii*, and catechins and theobromine had cysticidal effects. Despite the promising results, the clinical efficacy of *C. sinensis* SE for treatment of AK is unknown, as several preclinical and clinical studies are still needed to show a clinically significant benefit above the FDA-approved drugs used to treat patients with AK. Similarly, the doses tested in the present study at the in vitro level may fail to anticipate *C. sinensis* SE toxicity in humans. Therefore, future studies are required to investigate the *in vivo* toxicity and anti-acanthamoebic efficacy of *C. sinensis* SE and to elucidate the mechanisms leading to *A. castellanii* damage after exposure to *C. sinensis*. Efficacy of *C. sinensis* SE can be tied to its ability to penetrate into the affected ocular tissues and achieve a therapeutic concentration. Therefore, the pharmacokinetic profile of *C. sinensis* SE and its penetration into tissue during an active ocular infection, as in the case of AK, needs to be elucidated.

Funding

Lenu Fakae was supported by The Barineme and Dorathy Fakae Education Trust Fund for completion of his PhD studies.

Ethics statement

Not applicable.

Supplementary data

Fig. S1. Representative photographs of *A. castellanii* cysts at 72 h post-exposure to 312.5 – 5000 μg/mL *C. sinensis* SE using phase-contrast microscopy. (a) Control cyst culture treated with PGY. (b-f) Cysts treated with 312.5 μg/mL, 625 μg/mL, 1250 μg/mL, 2500 μg/mL and 5000 μg/mL *C. sinensis,* respectively. (d-f) 1250 μg/mL, 2500 μg/mL and 5000 μg/mL *C. sinensis* SE showed the presence of damaged cysts, with cytosol contents observed in the culture medium. Adhesion of trophozoites to the flask surface was inhibited by all *C. sinensis* concentrations, confirmed by gentle rocking of the culture plates. (b, c) Cultures treated with 312.5 μg/mL and 625 μg/mL, respectively, also showed some debris and damaged cysts but not as extensive as observed at the higher concentrations. X40 magnification. Scale bar, 200 μm.

Fig. S2. Flash column chromatography of *C. sinensis* SE, mobile phase 1. *C. sinensis* SE chromatograph with a mobile phase of 0.2% acetic acid in water + acetonitrile at a 91:9 ratio and water + acetonitrile at a 20:80 ratio, showing peaks representative of fractions with possible analytes present in *C. sinensis* SE. The fractions are represented as peaks at different retention times.

Fig. S3. Flash column chromatography of *C. sinensis* SE, mobile phase 2. *C. sinensis* SE chromatograph with a mobile phase of 0.1% formic acid in water and water + 0.1% formic acid in methanol, showing peaks representative of fractions with possible analytes present in *C. sinensis* SE. The fractions are represented as peaks at different retention times.

Fig. S4. Growth inhibitory effect of *C. sinensis* chemical components combined. The combined treatment included epigallocatechin-3-gallate (EGCG), epicatechin-3-gallate (ECG), epigallocatechin (EGC), epicatechin (EC), catechin, caffeine, theobromine, myricetin, theogallin, and kaempferol. Trophozoites were treated with 3.125 - 200 μM for 24, 48, and 72 h. No significant differences were detected between treated groups and negative control (PGY) at 24 h and 48 h, while only 50 μM, 100 μM and 200 μM showed significant decrease compared to PGY treatment. ****, $p \leq 0.0001$; ns: non-significant.

Fig. S5. Inhibition of encystation of *A. castellanii* exposed to two *C. sinensis* chemical components individually (a) Epigallocatechin-3-gallate (EGCG) and (b) Theobromine, and as a combination at a 1:1 ratio (c). EGCG and Theobromine encystation solutions were used at concentrations of 62.5 - 500 μM. All concentrations displayed 100% inhibition of encystation, with no significant difference between them and positive control (5 mM PMSF). ****, $p \leq 0.0001$; ns: non-significant.

CRediT authorship contribution statement

Lenu B. Fakae: Methodology, Investigation, Data curation, Writing – original draft. **Mohammad S.R. Harun:** Software, Data curation. **Darren Shu Jeng Ting:** Writing – review & editing, Investigation. **Harminder S. Dua:** Writing – review & editing. **Gareth W.V. Cave:** Methodology, Data curation, Software. **Xing-Quan Zhu:** Validation, Writing – review & editing. **Carl W. Stevenson:** Supervision, Validation, Writing – review & editing. **Hany M. Elsheikha:** Conceptualization, Validation, Visualization, Supervision, Writing – review & editing.

Declaration of Competing Interest

The authors declare that they have no known competing financial interests or personal relationships that could have appeared to influence the work reported in this paper.

Data Availability

Data will be made available on request.

Acknowledgments

We thank the University of Nottingham School of Life Sciences imaging unit (SLIM) for technical assistance.

Supplementary materials

Supplementary material associated with this article can be found, in the online version, at doi:10.1016/j.actatropica.2022.106729.

References

Avdagic, E., Chew, H.F., Veldman, P., Tu, E.Y., Jafri, M., Doshi, R., Boggild, A.K., Reidy, J.J., Farooq, A.V., 2021. Resolution of *Acanthamoeba* Keratitis with adjunctive use of oral Miltefosine. Ocul. Immunol. Inflamm. 29, 278–281. https://doi.org/10.1080/09273948.2019.1695853.

Alsam, S., Sissons, J., Jayasekera, S., Khan, N.A., 2005. Extracellular proteases of *Acanthamoeba castellanii* (encephalitis isolate belonging to T1 genotype) contribute to increased permeability in an in vitro model of the human blood-brain barrier. J. Infect. 51, 150–156. https://doi.org/10.1016/j.jinf.2004.09.001.

Anwar, A., Khan, N.A., Siddiqui, R., 2018. Combating *Acanthamoeba spp.* cysts: what are the options? Parasit. Vectors 11, 26. https://doi.org/10.1186/s13071-017-2572-z.

Bagshaw, R.J., Stewart, A.G., Smith, S., Carter, A.W., Hanson, J., 2020. The characteristics and clinical course of patients with scrub typhus and Queensland tick typhus infection requiring intensive care unit admission: a 23-year case series from Queensland, Tropical Australia. Am. J. Trop. Med. Hyg. 103, 2472. https://doi.org/10.4269/ajtmh.20-0780.

Benelli, R., Venè, R., Bisacchi, D., Garbisa, S., Albini, A., 2002. Anti-invasive effects of green tea polyphenol epigallocatechin-3-gallate (EGCG), a natural inhibitor of metallo and serine proteases. Biol. Chem. 383, 101–105. https://doi.org/10.1515/BC.2002.010.

Carnt, N.A., Subedi, D., Connor, S., Kilvington, S., 2020. The relationship between environmental sources and the susceptibility of *Acanthamoeba* keratitis in the United Kingdom. PLoS ONE 15, 0229681. https://doi.org/10.1371/journal.pone.0229681 e.

Dart, J.K.G., Saw, V.P.J., Kilvington, S., 2009. Acanthamoeba keratitis: diagnosis and treatment update 2009. Am. J. Ophthalmol. 148, 487–499. https://doi.org/10.1016/j.ajo.2009.06.009 e482.

Dickson, A., Cooper, E., Fakae, L.B., Wang, B., Chan, K.L.A., Elsheikha, H.M., 2020. In vitro growth- and encystation-inhibitory efficacies of matcha green tea and epigallocatechin gallate against *Acanthameoba castellanii*. Pathogens 9, 763. https://doi.org/10.3390/pathogens9090763.

Dodangeh, S., Niyyati, M., Kamalinejad, M., Lorenzo morales, J., Moshfe, A., Haghighi, A., Azargashb, E., 2018. In vitro activity of *Trigonella foenum graecum* seeds against a clinical strain of *Acanthamoeba* genotype T4. Iran J. Pharm. Res. 17, 661–667.

Dudley, R., Alsam, S., Khan, N.A., 2008. The role of proteases in the differentiation of *Acanthamoeba castellanii*. FEMS Microbiol. Lett. 286, 9–15. https://doi.org/10.1111/j.1574-6968.2008.01249.x.

Fakae, L.B., Stevenson, C.W., Zhu, X.Q., Elsheikha, H.M., 2020. In vitro activity of *Camellia sinensis* (green tea) against trophozoites and cysts of *Acanthamoeba castellanii*. Int. J. Parasitol. Drugs Drug Resist. 13, 59–72. https://doi.org/10.1016/j.ijpddr.2020.05.001.

Ferro, S., Coppellotti, O., Roncucci, G., Ben Amor, T., Jori, G., 2006. Photosensitized inactivation of *Acanthamoeba palestinensis* in the cystic stage. J. Appl. Microbiol. 101, 206–212. https://doi.org/10.1111/j.1365-2672.2006.02893.x.

Gu, B., Ding, Q., Xia, G., Fang, Z., 2009. EGCG inhibits growth and induces apoptosis in renal cell carcinoma through TFPI-2 overexpression. Oncol. Rep. 21, 635–640. https://doi.org/10.3892/or_00000266.

Hadas, E., Derda, M., Cholewinski, M., 2017a. Evaluation of the effectiveness of tea tree oil in treatment of *Acanthamoeba* infection. Parasitol. Res. 116, 997–1001. https://doi.org/10.1007/s00436-017-5377-2.

Hadas, E., Derda, M., Nawrot, J., Nowak, G., Thiem, B., 2017b. Evaluation of the amoebicidal activities of *Centaurea bella, Centaurea daghestanica, Rhaponticum pulchrum* and *Tanacetum vulgare* against pathogenic *Acanthamoeba spp.* Acta Pol. Pharm. 74, 1827–1832.

Hay, J., Kirkness, C.M., Seal, D.V., Wright, P., 1994. Drug resistance and *Acanthamoeba* Keratitis: the quest for alternative antiprotozoal chemotherapy. Eye 8, 555–563. https://doi.org/10.1038/eye.1994.137.

Katada, S., Yanagimoto, A., Matsui, Y., Hibi, M., Osaki, N., Kobayashi, S., Katsuragi, Y., 2020. Effect of tea catechins with caffeine on energy expenditure in middle-aged men and women: a randomized, double-blind, placebo-controlled, crossover trial. Eur. J. Nutr. 59, 1163–1170. https://doi.org/10.1007/s00394-019-01976-9.10.1007/s00394-019-01976-9.

Kaya, Y., Baldemir, A., Karaman, Ü., Ildız, N., Arıcı, Y.K., Kaçmaz, G., Kolören, Z., Konca, Y., 2019. Amebicidal effects of fenugreek (*Trigonella foenum-graecum*) against *Acanthamoeba* cysts. Food Sci. Nutr. 7, 563–571. https://onlinelibrary.wiley.com/doi/abs/10.1002/fsn3.849.

Kaynak, B., Koloren, Z., Karaman, U., 2018. Investigation of in vitro amoebicidal activities of *Ornithogalum sigmoideum* on *Acanthamoeba castellanii* cysts and trophozoites. Ann. Med. Res. 25, 709–715. https://doi.org/10.5455/annalsmedres.2018.07.145.

Khan, N.A., 2006. *Acanthamoeba*: biology and increasing importance in human health. FEMS Microbiol. Rev. 30, 564–595. https://doi.org/10.1111/j.1574-6976.2006.00023.x.

Khan, Y.A., Kashiwabuchi, R.T., Martins, S.A., Castro-Combs, J.M., Kalyani, S., Stanley, P., Flikier, D., Behrens, A., 2011. Riboflavin and ultraviolet light A therapy as an adjuvant treatment for medically refractive *Acanthamoeba* Keratitis report of 3 cases. Ophthalmology 118, 324–331. https://doi.org/10.1016/j.ophtha.2010.06.041.

Kofman, A., Guarner, J., 2022. Infections caused by free living amoebae. J. Clinical Microbiol. 60, e0022821 https://doi.org/10.1128/JCM.00228-21.

Lorenzo-Morales, J., Khan, N.A., Walochnik, J., 2015. An update on *Acanthamoeba* keratitis: diagnosis, pathogenesis and treatment. Parasite 22. https://doi.org/10.1051/parasite/2015010.

Lorenzo-Morales, J., Martin-Navarro, C.M., Lopez-Arencibia, A., Santana-Morales, M.A., Afonso-Lehmann, R.N., Maciver, S.K., Valladares, B., Martinez-Carretero, E., 2010. Therapeutic potential of a combination of two gene-specific small interfering RNAs against clinical strains of *Acanthamoeba*. Antimicrob. Agents Chemother. 54, 5151–5155. https://doi.org/10.1128/AAC.00329-10.

Mahboob, T., Azlan, A.M., Shipton, F.N., Boonroumkaew, P., Azman, N.S.N., Sekaran, S. D., Ithoi, I., Tan, T.C., Samudi, C., Wiart, C., Nissapatorn, V., 2017. Acanthamoebicidal activity of periglaucine A and betulinic acid from *Pericampylus glaucus* (Lam.) Merr. in vitro. Exp. Parasitol. 183, 160–166. https://doi.org/10.1016/j.exppara.2017.09.002.

Martín-Navarro, C.M., Lorenzo-Morales, J., Cabrera-Serra, M.G., Rancel, F., Coronado-Álvarez, N.M., Piñero, J.E., Valladares, B., 2008. The potential pathogenicity of chlorhexidine-sensitive *Acanthamoeba* strains isolated from contact lens cases from asymptomatic individuals in Tenerife, Canary Islands, Spain. J. Med. Microbiol. 57, 1399–1404. https://doi.org/10.1099/jmm.0.2008/003459-0.

Navarro-Martínez, M.D., Navarro-Perán, E., Cabezas-Herrera, J., Ruiz-Gómez, J., García-Cánovas, F., Rodríguez-López, J.N., 2005. Antifolate activity of epigallocatechin gallate against *Stenotrophomonas maltophilia*. Antimicrob. Agents Chemother. 49, 2914–2920. https://doi.org/10.1128/AAC.49.7.2914-2920.2005.

Ortega-Rivas, A., Padrón, J.M., Valladares, B., Elsheikha, H.M., 2016. *Acanthamoeba castellanii*: a new high-throughput method for drug screening in vitro. Acta Trop. 164, 95–99. https://doi.org/10.1016/j.actatropica.2016.09.006.

Said, D.G., Rallis, K.I., Al-Aqaba, M.A., Ting, D.S.J., Dua, H.S., 2021. Surgical management of infectious keratitis. Ocul. Surf. Press. https://doi.org/10.1016/j.jtos.2021.09.005.

Sanlier, N., Gokcen, B.B., Altuğ, M., 2018. Tea consumption and disease correlations. Trends Food Sci. Technol. 78, 95–106. https://doi.org/10.1016/j.tifs.2018.05.026.

Saoudi, S., Sifaoui, I., Chammem, N., Reyes-Batlle, M., Lopez-Arencibia, A., Pacheco-Fernandez, I., Pino, V., Hamdi, M., Jimenez, I.A., Bazzocchi, I.L., Pinero, J.E., Lorenzo-Morales, J., 2017. Anti-*Acanthamoeba* activity of Tunisian *Thymus capitatus* essential oil and organic extracts. Exp. Parasitol. 183, 231–235. https://doi.org/10.1016/j.exppara.2017.09.014.

Shankar, S., Suthakar, G., Srivastava, R.K., 2007. Epigallocatechin-3-gallate inhibits cell cycle and induces apoptosis in pancreatic cancer. Front. Biosci. 12, 5039–5051. https://doi.org/10.2741/2446.

Si, Z., Veldman, P.B., Reidy, J.J., Farooq, A.V., 2022. Severe Inflammatory response in a patient on oral miltefosine for *Acanthamoeba* Keratitis. Ocul. Immunol. Inflamm. 30, 1027–1028. https://doi.org/10.1080/09273948.2020.1854315.

Siddiqui, R., Aqeel, Y., Khan, N.A., 2016. The development of drugs against *Acanthamoeba* infections. Antimicrob. Agents Chemother. 60, 6441–6450. https://doi.org/10.1128/AAC.00686-16.

Sifaoui, I., Lopez-Arencibia, A., Martin-Navarro, C.M., Reyes-Batlle, M., Wagner, C., Chiboub, O., Mejri, M., Valladares, B., Abderrabba, M., Pinero, J.E., Lorenzo-Morales, J., 2017. Programmed cell death in *Acanthamoeba castellanii* Neff induced by several molecules present in olive leaf extracts. PLoS ONE 12, 12. https://doi.org/10.1371/journal.pone.0183795.

Srichairatanakool, S., Ounjaijean, S., Thephinlap, C., Khansuwan, U., Phisalpong, C., Fucharoen, S., 2006. Iron-chelating and free-radical scavenging activities of microwave-processed green tea in iron overload. Hemoglobin 30, 311–327. https://doi.org/10.1080/03630260600642666.

Thulasi, P., Saeed, H.N., Rapuano, C.J., Hou, J.H., Appenheimer, A.B., Chodosh, J., Kang, J.J., Morrill, A.M., Vyas, N., Zegans, M.E., Zuckerman, R., Tu, E.Y., 2021. Oral Miltefosine as salvage therapy for refractory *Acanthamoeba* Keratitis. Am. J. Ophthalmol. 223, 75–82. https://doi.org/10.1016/j.ajo.2020.09.048.

Ting, D.S.J., Ho, C.S., Deshmukh, R., Said, D.G., Dua, H.S., 2021a. Infectious keratitis: an update on epidemiology, causative microorganisms, risk factors, and antimicrobial resistance. Eye 35, 1084–1101. https://doi.org/10.1038/s41433-020-01339-3 (Lond).

Ting, D.S.J., Ho, C.S., Cairns, J., Elsahn, A., Al-Aqaba, M., Boswell, T., Said, D.G., Dua, H. S., 2021b. 12-year analysis of incidence, microbiological profiles and in vitro antimicrobial susceptibility of infectious keratitis: the Nottingham infectious keratitis study. Br. J. Ophthalmol. 105, 328–333. https://doi.org/10.1136/bjophthalmol-2020-316128.

Ting, D.S.J., Henein, C., Said, D.G., Dua, H.S., 2021c. Photoactivated chromophore for infectious keratitis-corneal cross-linking (PACK-CXL): a systematic review and meta-analysis. Ocul. Surf. 17, 624–634. https://doi.org/10.1016/j.jtos.2019.08.006.

Ting, D.S.J., Henein, C., Said, D.G., Dua, H.S., 2021d. Amniotic membrane transplantation for infectious keratitis: a systematic review and meta-analysis. Sci. Rep. 11, 13007. https://doi.org/10.1038/s41598-021-92366-x.

Wyganowska-Świątkowska, M., Matthews-Kozanecka, M., Matthews-Brzozowska, T., Skrzypczak-Jankun, E., Jankun, J., 2018. Can EGCG alleviate symptoms of down syndrome by altering proteolytic activity? Int. J. Mol. Sci. 19, 248. https://doi.org/10.3390/ijms19010248.

Yang, K., Gao, Z.Y., Li, T.Q., Song, W., Xiao, W., Zheng, J., Chen, H., Chen, G.H., Zou, H. Y., 2019. Anti-tumor activity and the mechanism of a green tea (*Camellia sinensis*) polysaccharide on prostate cancer. Int. J. Biol. Macromol. 122, 95–103. https://doi.org/10.1016/j.ijbiomac.2018.10.101.

Zainuddin, A., Hidayat, I.W., Kurnia, D., Ramadhanty, Z.F., Padilah, R., 2022. Prediction of the mechanism of action of catechin as superoxide anion antioxidants and natural antivirals for COVID-19 infection with in silico study. J. Adv. Pharm. Technol. Res. 13, 191–196. https://doi.org/10.4103/japtr.japtr_67_22.